Inorg. Chem. **2005**, *44*, 4747–4755

Dinuclear, Bishydrated Gd^{III} Polyaminocarboxylates with a Rigid Xylene Core Display Remarkable Proton Relaxivities

Jérôme Costa, Éva Tóth, Lothar Helm, and André E. Merbach*

Ecole Polytechnique Fédérale de Lausanne (EPFL), Laboratoire de Chimie Inorganique et Bioinorganique, EPFL-BCH, CH-1015 Lausanne, Switzerland

Received January 10, 2005

Two novel dinuclear Gd^{III} complexes have been synthesized, based on a xylene core substituted with diethylenetriamine-*N,N,N′′,N′′*-tetraacetate (DTTA) chelators in para or meta position. The complexes $[Gd_2(pX(DTTA)_2)(H_2O)_4]^{2-}$ and $[Gd_2(mX(DTTA)_2)(H_2O)_4]^{2-}$ both exhibit high complex stability (log $K_{GdL} = 19.1$ and 17.0, respectively), and a good selectivity for Gd^{III} against Zn^{II}, the most abundant endogenous metal ion (log $K_{ZnL} = 17.94$ and 16.19). The water exchange rate is identical within experimental error for the two isomers: $k_{ex}^{298} = (9.0 \pm 0.4) \times 10^6\ s^{-1}$ for $[Gd_2(pX(DTTA)_2)(H_2O)_4]^{2-}$ and $(8.9 \pm 0.5) \times 10^6\ s^{-1}$ for $[Gd_2(mX(DTTA)_2)(H_2O)_4]^{2-}$. It is very similar to the k_{ex}^{298} of the structural analogue, bishydrated $[Gd(TTAHA)(H_2O)_2]^{3-}$, and about twice as high as that of the monohydrated $[Gd(DTPA)(H_2O)]^{2-}$ ($TTAHA^{6-}$ = *N*-tris(2-aminoethyl)amine-*N′,N′,N′′,N′′,N′′′,N′′′*-hexaacetate; $DTPA^{5-}$ = diethylenetriamine-*N,N,N′,N′′,N′′*-pentaacetate). This relatively fast water exchange can be related to the presence of two inner sphere water molecules which decrease the stereorigidity of the inner sphere thus facilitating the water exchange process. At all frequencies, the water proton relaxivities ($r_1 = 16.79$ and 15.84 $mM^{-1}\ s^{-1}$ for the para and meta isomers, respectively; 25 °C and 20 MHz) are remarkably higher for the two dinuclear chelates than those of mononuclear commercial contrast agents or previously reported dinuclear Gd^{III} complexes. This is mainly the consequence of the two inner-sphere water molecules. In addition, the increased molecular size as compared to monomeric compounds associated with the rigid xylene linker between the two Gd^{III} chelating subunits also contributes to an increased relaxivity. However, proton relaxivity is still limited by fast molecular motions which also hinder any beneficial effect of the increased water exchange rate.

Introduction

Magnetic resonance imaging (MRI) has proven to be a highly efficient medical modality that has revolutionized clinical diagnosis. The progress of this technique, which was awarded the 2003 Nobel Prize for Physiology or Medicine, was made possible by the concomitant development of MRI contrast agents. By accelerating the nuclear relaxation of water protons in soft tissues, these drugs are able to enhance the intrinsic contrast and thus the anatomical resolution of the magnetic resonance images. Today, more than 30% of all MRI examinations use contrast enhancement, in majority produced by gadolinium(III) complexes of DTPA- or DOTA-type ligands (Figure 1).

Relaxivity is a gauge of MRI contrast agent efficiency. It is defined as the paramagnetic enhancement of the longitudinal proton relaxation rate and is referred to 1 mM Gd^{III} concentration. While actual contrast agents display relaxivities of around 4−5 $mM^{-1}\ s^{-1}$ at magnetic fields currently used in the clinics, the Solomon−Bloembergen−Morgan theory predicts an over 20-fold relaxivity gain on simultaneous optimization of the key factors: electron spin relaxation, water exchange, and molecular reorientation.[1] On a rational basis, the electronic relaxation of the paramagnetic center is still hard to influence. The inner-sphere water exchange rate has been recently shown to attain optimal values when steric compression is created around the water binding site in the chelate.[2,3] Finally, the reorientation of the Gd−H water proton vector can be optimized (slowed) by

* Corresponding author. Telephone: +41 21 693 9871. Fax: +41 21 693 9875. E-mail: andre.merbach@epfl.ch.

(1) Tóth, É.; Helm, L.; Merbach, A. E. Relaxivity of Gadolinium(III) Complexes: Theory and Mechanism. In *The Chemistry of Contrast Agents in Medical Magnetic Resonance Imaging*; Tóth, É., Merbach, A. E., Eds.; Wiley: Chichester, U.K., 2001.
(2) Ruloff, R.; Tóth, É.; Scopelliti, R.; Tripier, R.; Handel, H.; Merbach, A. E. *Chem. Commun.* **2002**, 2630.
(3) Laus, S.; Ruloff, R.; Tóth, É.; Merbach, A. E. *Chem. Eur. J.* **2003**, *9*, 3555.

10.1021/ic0500309 CCC: $30.25
Published on Web 05/19/2005

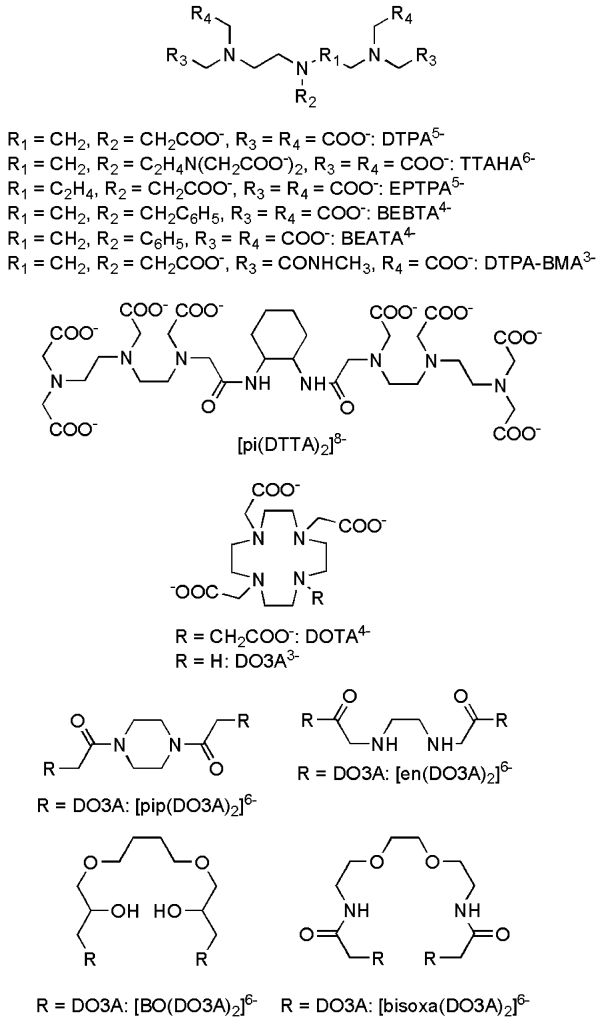

Figure 1. Structures of the ligands discussed in the text.

increasing the molecular size of the gadolinium(III) chelate, and maintaining a sufficient internal rigidity of the system.

Dinuclear complexes of Gd_2L type, derived from the DOTA and DTPA monomers have been reported in the past years.[4−8] On the basis of their increased molecular weight, these complexes were expected to have a slower tumbling time and thus a higher proton relaxivity. However, due to fast local motions of the Gd−water proton vector, induced by the flexibility of the linker between the two Gd^{III} chelating units, the relaxivity gain was less than expected. In addition, the water exchange rate was not improved with respect to the parent monomer chelates. Recently we reported a self-assembled dinuclear Gd^{III} complex with an $Fe^{II}(terpy)_2$ core that possesses an extreme rigidity and, as a consequence, a remarkably high proton relaxivity in comparison to Gd^{III} chelates of similar molecular weight.[9]

Here we report the synthesis of two, para- and meta-substituted xylene ligands, where the metal chelating entity is a diethylenetriamine-*N*,*N*,*N*′′,*N*′′-tetraacetate (DTTA) subunit, derived from DTPA by removing the central acetate group. These new $[pX(DTTA)_2]^{8-}$ and $[mX(DTTA)_2]^{8-}$ ligands can coordinate two Gd^{III} ions each to form the $[Gd_2(pX(DTTA)_2)(H_2O)_4]^{2-}$ and $[Gd_2(mX(DTTA)_2)(H_2O)_4]^{2-}$ complexes. The aromatic linker between the DTTA subunits is expected to induce rigidity, thus high relaxivity for the chelates, while the N_3O_4 donor set of DTTA should guarantee an increase in the water exchange rate. Moreover, the lanthanide ion can still accommodate two inner-sphere water molecules which doubles the inner-sphere contribution to proton relaxivity.

The three main influencing factors of proton relaxivity (water exchange, rotation and electronic relaxation) have been described for the two dinuclear complexes by a multiple-field, variable temperature ^{17}O NMR and ^1H NMRD study. In addition, we have determined ligand protonation and complex stability constants for various metal ions with the aim of assessing safety considerations for the two gadolinium(III) chelates as potential medical MRI contrast agents.

Experimental Section

Ligand Syntheses. Reagents and solvents were purchased from commercial sources with the highest quality grade and were used without further purification. α,α′-Diamino-*p*-xylene (respectively α,α′-diamino-*m*-xylene) (566.6 mg, 4.16 mmol) was dissolved in CH_3CN (110 mL). K_2CO_3 (5.75 g, 41.6 mmol) was added, and an excess solution of *N*,*N*-bis[(*tert*-butoxycarbonyl)methyl]-2-bromoethylamine, synthesized according to the literature[10] (6.59 g, 18.7 mmol) in CH_3CN (45 mL), was slowly dropped into the reaction solution. After stirring at room temperature for 24 h, the mixture was filtered and evaporated. CH_2Cl_2 (100 mL) was added to the solution, which was filtered and evaporated to afford an orange oil. After silica gel chromatography purification (95/5, CH_2Cl_2/CH_3OH), the orange oil was dissolved in 20 mL of 6 M HCl and the hydrolysis was carried out with stirring under reflux during 12 h. After filtration, the solvent was removed under reduced pressure. The solid was dissolved in a minimum of water and loaded onto a cation-exchange column (Dowex 50W-X2, H^+ form, 100 g). The column was washed with H_2O until neutral pH, and the product was eluted with HCl gradient (0.1−4.0 M). The desired product was collected with 3.0 M HCl as a colorless solution. The eluate was evaporated under reduced pressure to complete dryness and redissolved in H_2O. Evaporation and redissolution were repeated twice more, and the final product was obtained as a white powder. For $[pX(DTTA)_2]^{8-}$: 878.3 mg (0.87 mmol, 20.9% yield). ^1H NMR (200 MHz, D_2O [HDO 4.80 ppm], pH = 2.5): δ 3.48 (m, 16H), 3.85 (s, 16H), 4.42 (s, 4H), 7.60 (s, 4H). MS (ESI): *m*/*z* 773.3 [*M* + H]$^+$. Anal. Calcd for $C_{32}H_{48}N_6O_{16}\cdot 6HCl\cdot H_2O$: C, 38.07; H, 5.59; N, 8.32. Found (Service de Microanalyse, University of Geneva): C, 38.26; H, 5.88; N, 8.33. For $[mX(DTTA)_2]^{8-}$: 476.8 mg (0.49 mmol, 11.7% yield). ^1H NMR (200 MHz, D_2O [HDO, 4.80 ppm], pH = 3.2): δ 3.24 (m, 8H), 3.48 (m, 8H), 3.75 (s, 16H), 4.11 (s, 4H), 7.51 (s, 3H), 7.56 (s, 1H). MS (ESI): *m*/*z* 773.3 [*M* + H]$^+$. Anal. Calcd for $C_{32}H_{48}N_6O_{16}\cdot 5HCl\cdot H_2O$: C, 39.50; H, 5.70; N, 8.64. Found: C, 39.24; H, 5.76; N, 8.78.

Sample Preparation. The aqueous solutions of $[Ln_2(pX(DTTA)_2)(H_2O)_4]^{2-}$ and $[Ln_2(mX(DTTA)_2)(H_2O)_4]^{2-}$ (Ln^{III} = Gd^{III}, Eu^{III})

(4) Powell, D. H.; Dhubhghaill, O. M. N.; Pubanz, D.; Helm, L.; Lebedev, Y. S.; Schlaepfer, W.; Merbach, A. E. *J. Am. Chem. Soc.* **1996**, *118*, 9333.
(5) Tóth, É.; Vauthey, S.; Pubanz, D.; Merbach, A. E. *Inorg. Chem.* **1996**, *35*, 3375.
(6) Lee, T.-M.; Cheng, T.-H.; Ou, M.-H.; Chang, C. A.; Liu, G.-C.; Wang, Y.-M. *Magn. Reson. Chem.* **2004**, *42*, 329.
(7) Bovens, E.; Hoefnagel, M. A.; Boers, E.; Lammers, H.; van Bekkum, H.; Peters, J. A. *Inorg. Chem.* **1996**, *35*, 7679.
(8) Zitha-Bovens, E.; Vander Elst, L.; Muller, R. N.; van Bekkum, H.; Peters, J. A. *Eur. J. Inorg. Chem.* **2001**, 3101.
(9) Ruloff, R.; van Koten, G.; Merbach, A. E. *Chem. Commun.* **2004**, 842.
(10) Williams, M. A.; Rapoport, H. *J. Org. Chem.* **1993**, *58*, 1151.

were prepared by mixing $Ln(ClO_4)_3$ and ligand solutions in stoechiometric amounts. A slight ligand excess was used, and the pH was adjusted to about 6 by adding NaOH solution. The absence of free metal was checked with the xylenol orange test.[11] All gadolinium-containing samples used for the ^{17}O NMR measurements had 2% $H_2{}^{17}O$ enrichment (IsoTrade GmbH, Mönchengladbach, Germany).

Potentiometry. pH potentiometric titrations were performed to determine the protonation constants of the ligands $[pX(DTTA)_2]^{8-}$ and $[mX(DTTA)_2]^{8-}$ ($C_L = 3$ mM) and the stability constants of their complexes with various metals (Gd^{III}, Zn^{II}, Ca^{II}; $C_L = 3$ mM, $C_M = 6$ mM; $I = 0.1$ M $(CH_3)_4NCl$, titrated with 50 mM $(CH_3)_4NOH$). The titrations were carried out using 3 mL sample volumes, in a thermostated (25 ± 0.2 °C) glass-jacketed vessel with a magnetic stirrer (in an N_2 atmosphere to avoid the effects of CO_2), with a Metrohm Dosimat 665 automatic buret and a combined glass electrode (C14/02-SC, reference electrode part Ag/AgCl in 3 M KCl, Moeller Scientific Glass Instruments, Switzerland) connected to a Metrohm 692 pH/ion meter. The hydrogen ion concentration was calculated from the measured pH values by using a correction term, obtained as the difference between the measured and calculated pH values in a titration of HCl (0.1 M) with standardized KOH, as suggested by Irving.[12]

UV−Vis Spectrophotometry. The absorbance spectra were recorded on a Perkin-Elmer Lambda 19 spectrometer in thermostated cells at 16.7 and 75.3 °C for $[Eu_2(pX(DTTA)_2)(H_2O)_4]^{2-}$ and 13.2 and 80.3 °C for $[Eu_2(mX(DTTA)_2)(H_2O)_4]^{2-}$ ($C_{Eu} \approx 25$ mM for both complexes, pH = 5.8). The measurements were done with a 10 cm optical path length at $\lambda = 576.5-582.0$ nm.

^{17}O NMR Measurements. ^{17}O NMR spectra of $[Gd_2(pX(DTTA)_2)(H_2O)_4]^{2-}$ ($C_{Gd} = 23.38$ mmol kg^{-1}, pH = 5.57) and $[Gd_2(mX(DTTA)_2)(H_2O)_4]^{2-}$ ($C_{Gd} = 42.35$ mmol kg^{-1}, pH = 5.82) were recorded at variable temperature on Bruker DPX-400 (9.4 T, 54.2 MHz) and Bruker Avance-200 (4.7 T, 27.1 MHz) spectrometers. Bruker B-VT 3000 temperature control units were used to maintain a constant temperature, which was measured by a substitution technique.[13] Transverse and longitudinal ^{17}O relaxation rates and chemical shifts were measured for temperatures between 276.6 and 370.7 K. The samples were sealed in glass spheres adapted for 10 mm NMR tubes to avoid susceptibility corrections of the chemical shift.[14] The longitudinal and transverse relaxation times, T_1 and T_2, were obtained with the inversion−recovery[15] and the Carr−Purcell−Meiboom−Gill[16] spin−echo techniques, respectively. Acidified water ($HClO_4$, pH = 3.7) was used as an external reference.

^1H NMRD Relaxivity. Water proton relaxation rates of aqueous solutions containing $[Gd_2(pX(DTTA)_2)(H_2O)_4]^{2-}$ ($C_{Gd} = 5.31$ mM, pH = 5.51) and $[Gd_2(mX(DTTA)_2)(H_2O)_4]^{2-}$ ($C_{Gd} = 8.15$ mM, pH = 5.77) were measured at 293.2, 298.2, and 310.2 K on a Stelar Spinmaster FFC relaxometer (fast field cycling, 7×10^{-4} to 0.47 T, corresponding to a proton Larmor frequency range of 0.01−20 MHz) equipped with a VTC90 temperature control unit, on a Bruker Minispec console connected to 0.94 T (40 MHz), and 1.41 T (60 MHz) permanent magnets, on a Bruker Avance-200 console connected to 1.18 T (50 MHz), 2.35 T (100 MHz), and 4.7 T (200 MHz) cryomagnets and on a Bruker DPX-400 spectrometer (9.4 T, 400 MHz). The samples were placed in cylindrical tubes. The diamagnetic corrections to the ^1H longitudinal relaxation rates were 0.44 s^{-1} (293.2 K), 0.37 s^{-1} (298.2 K), and 0.33 s^{-1} (310.2 K).

Data Analysis. The simultaneous least-squares fit of ^{17}O NMR and ^1H NMRD data and the fit of the UV−vis absorbance spectra were performed by the Visualiseur/Optimiseur programs on a Matlab platform, version 6.5.[17,18] The thermodynamic equilibrium constants and potentiometric protonation constants were calculated with PSEQUAD.[19] The errors of the fitted parameters correspond to one standard deviation.

Results and Discussion

Synthesis. Both $[pX(DTTA)_2]^{8-}$ and $[mX(DTTA)_2]^{8-}$ ligands are derived from the tripod $TTAHA^{6-}$ (Figure 1). The X-ray crystal structure of $[C(NH_2)_3]_3[Gd(TTAHA)]\cdot 9H_2O$ revealed that the gadolinium(III) is coordinated by the seven atoms of the N_3O_4 donor set of the ligand. Two additional oxygen atoms from one carboxylate group of a neighboring complex complete the coordination cage around the lanthanide ion.[20] In solution, the bridging oxygens of the neighboring complex are replaced by two water molecules.[21] Substitution of the third "useless" pending arm of $TTAHA^{6-}$ by a xylene group offers the possibility to introduce a second metal coordinating DTTA subunit, either in para or in meta position, in one single molecule (Scheme 1). The ligands were synthesized starting from the aromatic core, by nucleophilic substitution of their amino endings with the *N*,*N*-bis[(*tert*-butoxycarbonyl)methyl]-2-bromoethylamine building block.[10] Attempts to obtain the corresponding ortho isomer were unsuccessful, probably due to steric hindrance.

Protonation and Stability Constants. In addition to high water solubility and low osmolality that are required for tolerance reasons, it is primordial that the metal chelates used as MRI contrast agents do not dissociate into toxic free metal ion and ligand species once injected into the body. The thermodynamic stability of a metal complex is given by the stability constant K_{ML} following eq 1:

$$K_{ML} = \frac{[ML]}{[M][L]} \tag{1}$$

where [M], [L], and [ML] are the equilibrium concentrations of the metal ion, the deprotonated ligand, and the complex, respectively. At low pH, protonation of the complexes may have to be taken into account. It is characterized by the complex protonation constants K_{MH_iL}, as expressed in eq 2:

$$K_{MH_iL} = \frac{[MH_iL]}{[MH_{i-1}L][H^+]} \text{ for } i = 1,2,... \tag{2}$$

(11) Brunisholz, G.; Randin, M. *Helv. Chim. Acta* **1959**, *42*, 1927.
(12) Irving, H. M.; Miles, M. G.; Pettit, L. D. *Anal. Chim. Acta* **1967**, *38*, 475.
(13) Ammann, C.; Meier, P.; Merbach, A. E. *J. Magn. Reson.* **1982**, *46*, 319.
(14) Hugi, A. D.; Helm, L.; Merbach, A. E. *Helv. Chim. Acta* **1985**, *68*, 508.
(15) Vold, R. L.; Waugh, J. S.; Klein, M. P.; Phelps, D. E. *J. Chem. Phys.* **1968**, *48*, 3831.
(16) Meiboom, S.; Gill, D. *Rev. Sci. Instrum.* **1958**, *29*, 688.
(17) Yerly, F. *VISUALISEUR 2.3.4*; Université de Lausanne: Lausanne, Switzerland, 1999.
(18) Yerly, F. *OPTIMISEUR 2.3.4*; Université de Lausanne: Lausanne, Switzerland, 1999.
(19) Zekany, L.; Nagypal, I. *Computational Methods for Determination of Formation Constants*; Plenum Press: New York, 1985.
(20) Ruloff, R.; Gelbrich, T.; Sieler, J.; Hoyer, E.; Beyer, L. *Z. Naturforsch., B: Chem. Sci.* **1997**, *52*, 805.
(21) Ruloff, R.; Muller, R. N.; Pubanz, D.; Merbach, A. E. *Inorg. Chim. Acta* **1998**, *275−276*, 15.

Scheme 1. Synthesis of the $[pX(dtta)_2]^{8-}$ and $[mX(dtta)_2]^{8-}$ Ligands[a]

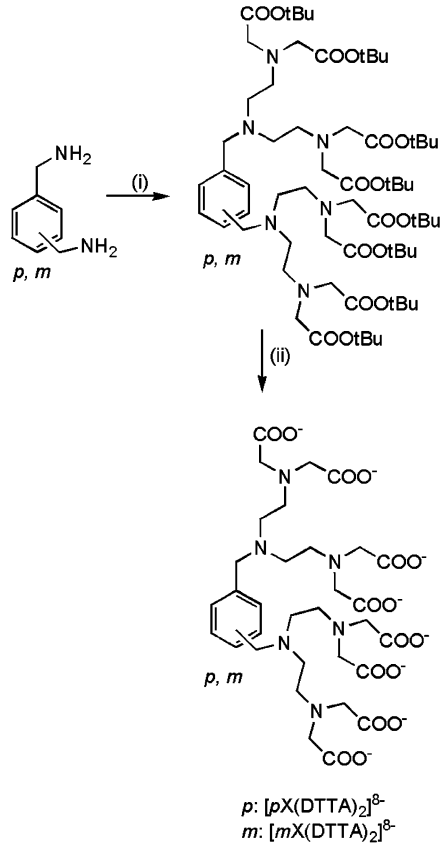

[a] Reagents and conditions: (i) $4BrC_2H_4N(CH_2COOtBu)_2$, K_2CO_3, CH_3CN, room temperature, 24 h; (ii) HCl 6 M, reflux, 12 h.

To calculate a stability constant, the protonation constants of the ligand, K_i as defined by eq 3, are also required:

$$K_i = \frac{[H_iL]}{[H_{i-1}L][H^+]} \qquad (3)$$

The stepwise protonation constants of the ligands $[pX(DTTA)_2]^{8-}$ and $[mX(DTTA)_2]^{8-}$, as well as the stability constants of their complexes formed with different metals (Gd^{III}, Zn^{II}, Ca^{II}) were obtained by potentiometric titration in the 2−12 pH range (Figure 2 for $[pX(DTTA)_2]^{8-}$ and Supporting Information for $[mX(DTTA)_2]^{8-}$). The constants and the standard deviations are summarized in Table 1.

Due to the distance between the two DTTA subunits in both ligands, we assumed that protonation occurs independently on both subunits (calculation of independent protonation constants for the two sets of sites was not possible). The system can therefore be regarded as two R-$DTTA^{4-}$ entities. This assumption is likely more valid for the para than for the meta isomer, where a slight influence of one DTTA subunit on the protonation (or metal complexation) of the other cannot be totally ruled out. On the other hand, inductive or mesomeric effects arising from the difference in para and meta substitutions that would affect the protonation constants of the pending DTTA entities are very unlikely, since the methylene group, intercalated between the aromatic ring and the polyaminocarboxylate acts as a "buffer" and quenches such effects.

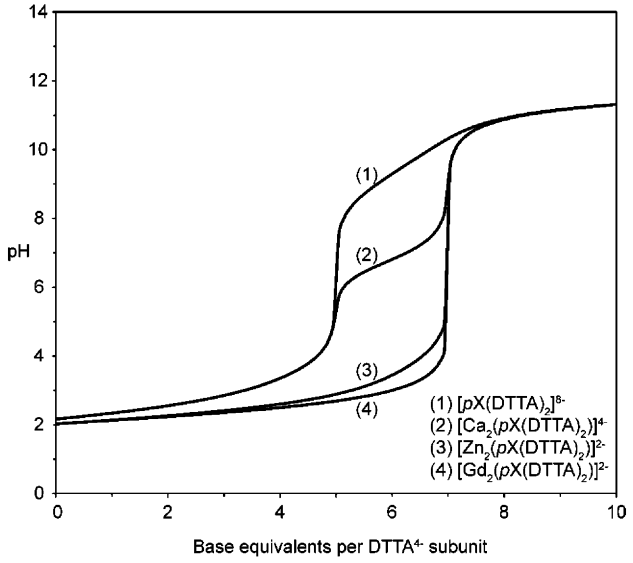

Figure 2. Titration curves (T = 25 °C, I = 0.1 M $(CH_3)_4NCl$) of the $[pX(DTTA)_2]^{8-}$ ligand and its Gd^{III}, Zn^{II} and Ca^{II} complexes.

The protonation constants for $[pX(DTTA)_2]^{8-}$ and $[mX(DTTA)_2]^{8-}$ ligands are intermediate between those of $DTPA^{5-}$ and $TTAHA,^{6-}$ both bearing electron-withdrawing substituents on the central nitrogen atom, and the log K_i values of $BEBTA,^{4-}$ which has a benzyl electron-donor group (see Figure 1 for the ligand structures and Table 1 for the log K_i values). The first protonation step likely occurs on the central nitrogen, while the second log K_i corresponds to the protonation of one of the terminal nitrogens, with displacement of the first proton from the central to the other terminal nitrogen, as it was demonstrated by ^1H NMR titration on $DTPA^{5-}$ and EPTPA.[5,22,23] At this stage, two protonated terminal nitrogens and four deprotonated carboxylates stabilize the whole system by internal hydrogen bridges. The two subsequent log K_i values correspond to the protonation of carboxylate groups. These log K_i values are different from those of the penta- and hexacarboxylate $DTPA^{5-}$ and TTAHA;[6,24,25] however, they are very similar to the log K_i values obtained for the tetracarboxylate $BEBTA^{4-}$ ligand.[26]

The stability constant of $[Gd_2(pX(DTTA)_2)(H_2O)_4]^{2-}$, log K_{GdL}, is high and comparable to that of $[Gd(TTAHA)(H_2O)_2]^{3-}$ and $[Gd(BEBTA)(H_2O)_2]^{2-}$, while the log K_{GdL} of $[mX(DTTA)_2]^{8-}$ is slightly lower. In comparison to the commercial contrast agent $[Gd(DTPA)(H_2O)]^{2-}$, the replacement of one anionic carboxylate donor group in the ligand by a nonionic xylene linker results in a diminution of the stability constant by 3−4 orders of magnitude. This is a clear consequence of the reduced number of donor atoms in the heptadentate $DTTA^{4-}$ as compared to the octadentate $DTPA.^{5-}$ Removal of the methylene group between the

(22) Wang, Y.-M.; Lee, C.-H.; Liu, G.-C.; Sheu, R.-S. *J. Chem. Soc., Dalton Trans.* **1998**, 4113.
(23) Letkeman, P.; Martell, A. E. *Inorg. Chem.* **1979**, *18*, 1284.
(24) *IUPAC Stability Constants 1.05*; Academic Software and K. J. Powell: Yorks, UK, 1999.
(25) Ruloff, R.; Arnold, K.; Beyer, L.; Dietze, F.; Gründer, W.; Wagner, M.; Hoyer, E. *Z. Anorg. Allg. Chem.* **1995**, *621*, 807.
(26) Vasil'eva, V. F.; Lavrova, O. Y.; Dyatlova, N. M.; Yashunskii, V. G. *Zh. Obshch. Khim.* **1966**, *36*, 1724.

Table 1. Protonation and Stability Constants for Various Ligands L and Their Gd^{III}, Zn^{II}, and Ca^{II} Complexes (T = 25 °C, I = 0.1 M $(CH_3)_4NCl$)

	L = $[p$X(DTTA$_2$]$^{8-}$	L = $[m$X(DTTA$_2$]$^{8-}$	L = TTAHA^{6-} [a]	L = DTPA^{5-} [b]	L = BEBTA^{4-} [c]
log K_1	9.84(3)	9.45(3)	10.66	10.41	9.05
log K_2	8.80(3)	8.12(3)	8.56	8.37	7.99
log K_3	3.52(4)	3.97(4)	8.38	4.09	3.98
log K_4	2.40(5)	2.70(3)	2.92	2.51	2.52
log K_5			2.39	2.04	
log K_6			2.0		
log K_{GdL}	19.1(1)	17.0(1)	19.0	22.5	17.50
log K_{GdHL}	2.1(1)	3.2(1)	8.3	1.8	
log K_{ZnL}	17.94(1)	16.19(3)	18.91	18.29	
log K_{ZnHL}	3.76(1)	4.24(2)	8.01	5.6	
log K_{ZnH2L}			3.68		
log K_{ZnH3L}			2.33		
log K_{CaL}	8.27(2)	7.55(2)	9.73	10.75	
log K_{CaHL}	6.07(9)	5.90(8)	8.64	6.11	

[a] I = 0.1 M KCl.[25,53] [b] I = 0.1 M KCl.[24] [c] No indication of I.[26]

Table 2. pM Values of GdL Complexes under Physiologically Relevant Conditions (pH 7.4; $[Gd]_{total}$ = 1 μM; $[L]_{total}$ = 10 μM)[a]

L	pGd	ref
DOTA^{4-} [b]	19.2	54
DTPA^{5-} [b]	19.1	24
BEBTA^{4-}	16.1	26
DTPA-BMA^{3-} [b]	15.8	28
TTAHA^{6-}	15.5	25
$[p$X(DTTA$_2$]$^{8-}$	16.2	this work
$[m$X(DTTA$_2$]$^{8-}$	15.1	this work

[a] For ligand structures, see Figure 1. [b] Ligands of commercial contrast agents.

phenyl ring and the DTTA subunit would maintain the gadolinium complexing N_3O_4 donor set and increase the rigidity of the system (an important feature for relaxivity considerations). However, it would drastically reduce the stability of the metal−ligand system. Indeed, Tse and Powell observed a remarkable decrease of log K_{GdL} from 17.50 to 15.42 on going from BEBTA^{4-} to BEATA,$^{4-}$ due to the replacement of the electron-donor benzyl group by an electron-withdrawing phenyl.[27]

Physiologically more relevant information on complex stability is provided by the pM values. The pM, usually calculated for pH 7.4, $[Gd]_{total}$ = 1 μM, and $[L]_{total}$ = 10 μM, expresses the influence of the ligand basicity and the protonation of the complex. A higher pM value means higher complex stability under these conditions. Table 2 shows pGd values for several, MRI relevant, Gd^{III} complexes. The pGd of both $[Gd_2(p\text{X(DTTA)}_2)(H_2O)_4]^{2-}$ and $[Gd_2(m\text{X(DTTA)}_2)(H_2O)_4]^{2-}$ is comparable to that of [Gd(DTPA-BMA)(H_2O)], a commercial MRI contrast agent.[28]

During an MRI examination, the Gd^{III} complex is injected into the blood stream of the patient, a chemically complex system with various endogenous substances (metal ions and biological ligands). Competition between Gd^{III} and endogenous metal ions must therefore be considered for toxicological reasons. For both $[p\text{X(DTTA)}_2]^{8-}$ and $[m\text{X(DTTA)}_2]$,[8−] the stability constants are higher with Gd^{III} than with the endogenous Zn^{II} or Ca^{II} (Table 1). The selectivity of both para and meta ligands for Gd^{III} over other metal ions (defined as $\log(K_{GdL}/K_{ML})$, M = Zn^{II}, Ca^{II}) is larger than that of TTAHA,$^{6-}$ especially for Zn^{II} which is the most abundant endogenous metal ion with an estimated concentration of 10^{-5} M in the plasma.[29] It has also to be mentioned that, in addition to thermodynamic stability, kinetic inertness of the Gd^{III} complexes is also primordial for safe in vivo application.

UV−Vis Spectrophotometry. The UV−vis absorbance spectrum, and in particular the $^7F_0 \rightarrow {}^5D_0$ transition band of Eu^{III} (577.5−581.5 nm) is very sensitive to the coordination environment of the lanthanide ion[30,31] and is often used to test the presence of differently coordinated species.[31] Both $[Eu_2(p\text{X(DTTA)}_2)(H_2O)_4]^{2-}$ and $[Eu_2(m\text{X(DTTA)}_2)(H_2O)_4]^{2-}$ have a single, temperature-invariant absorption band in this region (see Supporting Information), which proves the absence of a hydration equilibrium in solution within the temperature range studied (13.2−80.3 °C). By analogy, similar hydration mode (no hydration equilibrium) was assumed for the Gd^{III} corresponding complexes.

^{17}O NMR and ^{1}H NMRD. With the objective of determining parameters for water exchange, rotation, electronic relaxation, and proton relaxivity, we measured ^{17}O relaxation rates and chemical shifts and ^{1}H relaxation rates at different temperatures on aqueous solutions of the two dinuclear complexes. The experimental ^{17}O NMR and ^{1}H NMRD data were analyzed simultaneously[4] (for equations, refer to Appendix in Supporting Information) and are shown together with the fitted curves in Figure 3.

The water exchange rate $k_{ex} = 1/\tau_m$ is directly determining the reduced transverse relaxation rates in the slow-exchange region, at low temperatures, where $1/T_{2r}$ increases with temperature. At high temperatures (above 300 K), an inverse tendency is observed: $1/T_{2r}$ is decreasing with temperature. In this fast-exchange region, $1/T_{2r}$ is determined by the transverse relaxation rate of the bound water oxygen, which itself is influenced by k_{ex}, the longitudinal electronic relaxation rate $1/T_{1e}$, and the hyperfine or scalar coupling constant, $A/\hbar$. The reduced ^{17}O chemical shifts, $\Delta\omega_r$, are determined by $A/\hbar$ and, to a small extent, by an outer-sphere contribution characterized by C_{OS}, set to the common value

(27) Tse, P.-K.; Powell, J. E. *Inorg. Chem.* **1985**, *24*, 2727.
(28) Paul-Roth, C.; Raymond, K. N. *Inorg. Chem.* **1995**, *34*, 1408.
(29) May, P. M.; Linder, P. W.; Williams, D. R. *J. Chem. Soc., Dalton Trans.* **1977**, 588.
(30) Geier, G.; Jørgensen, C. K. *Chem. Phys. Lett.* **1971**, *9*, 263.
(31) Graeppi, N.; Powell, D. H.; Laurenczy, G.; Zékány, L.; Merbach, A. E. *Inorg. Chim. Acta* **1995**, *235*, 311.

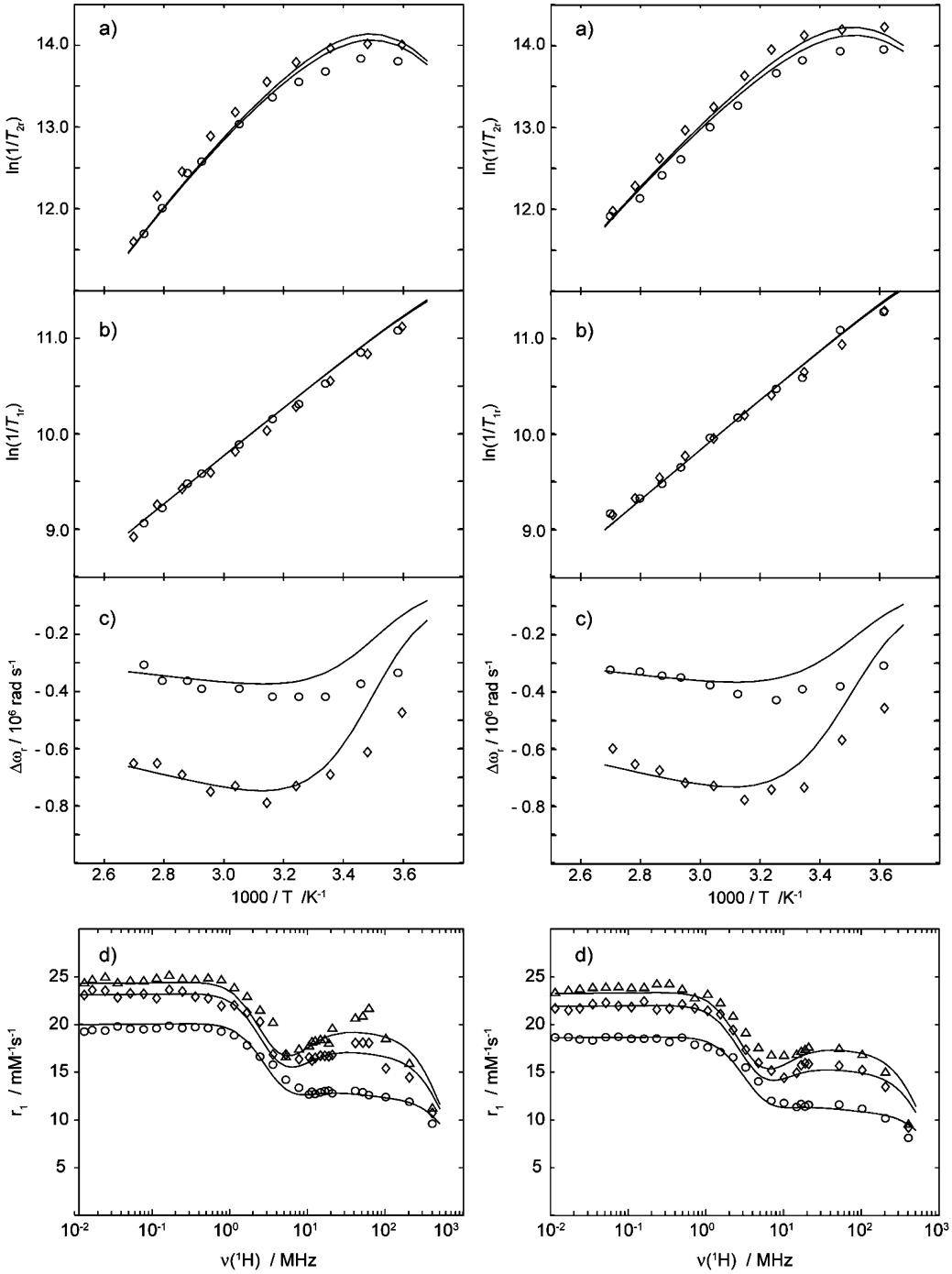

Figure 3. $[Gd_2(pX(DTTA)_2)(H_2O)_4]^{2-}$ (left boxes) and $[Gd_2(mX(DTTA)_2)(H_2O)_4]^{2-}$ (right boxes) temperature dependence of reduced (a) transverse $1/T_{2r}$ and (b) longitudinal $1/T_{1r}$ ^{17}O relaxation rates; (c) ^{17}O chemical shifts $\Delta\omega_r$ at $B = 4.7$ T (○) and 9.4 T (◇); (d) ^1H NMRD profiles at 20 (△), 25 (◇), and 37 °C (○). The lines represent curves fitted to the experimental points.

of 0.1.[32,33] The measured ^{17}O longitudinal relaxation rates, $1/T_{1r}$, lie in the fast-exchange region. $1/T_1$ of the water bound to Gd^{III} complexes in solution is dominated by dipole−dipole and quadrupolar relaxation mechanisms. The reduced rates, $1/T_{1r}$, are determined by the rotational correlation time for the Gd^{III}−O vector, τ_{RO} (and its activation energy, E_R), the quadrupolar coupling constant, $\chi(1 + \eta^2/3)^{1/2}$, and the Gd^{III}−oxygen distance, r_{GdO}.

The longitudinal ^1H relaxation rates were measured at three different temperatures and normalized to millimolar Gd^{III} concentration to obtain the longitudinal proton relaxivity, r_1, in mM^{-1} s^{-1}. The ^1H NMRD profiles are shown in Figure 3. The overall shape of the profiles presents a plateau at low frequencies (below 1 MHz) and a little relaxivity hump between 10 and 200 MHz.

Electronic relaxation rates $1/T_{ie}$ ($i = 1, 2$) influence both ^{17}O and ^1H NMR relaxation in Gd^{III} complexes and are generally governed by the zero-field splitting (ZFS) term.[34−36] Powell's approach[4] based on the Solomon−Bloembergen−

(32) Micskei, K.; Helm, L.; Brücher, E.; Merbach, A. E. *Inorg. Chem.* **1993**, *32*, 3844.
(33) González, G.; Powell, D. H.; Tissières, V.; Merbach, A. E. *J. Phys. Chem.* **1994**, *98*, 53.

Table 3. Parameters Obtained for $[Gd_2(pX(dtta)_2)(H_2O)_4]^{2-}$, $[Gd_2(mX(dtta)_2)(H_2O)_4]^{2-}$, and Parent Gd^{III} Chelates from the Analysis of ^{17}O NMR and ^1H NMRD Data[a]

	L = *p*X(DTTA)$_2$	L = *m*X(DTTA)$_2$	L = TTAHA[b]	L =DTPA[c]
ΔH (kJ mol^{-1})	45.4 ± 1.3	39.2 ± 1.3	40.4	51.6
ΔS (J mol^{-1} K^{-1})	+40.7 ± 4.8	+23.6 ± 4.8	+23.3	+53.0
k^{298}_{ex} (10^6 s^{-1})	9.0 ± 0.4	8.9 ± 0.5	8.6	3.3
τ^{298}_{RO} (ps)	278 ± 7	289 ± 7	82	58
E_r (kJ mol^{-1})	20.9 ± 0.9	21.8 ± 0.7	19.9	17.3
$A/\hbar$ (10^6 rad s^{-1})	−3.6 ± 0.1	−3.4 ± 0.1	−3.5	−3.8
τ^{298}_{v} (ps)	34.0 ± 0.5	29.2 ± 0.7	25	25
Δ^2 (10^{20} s^{-2})	0.16 ± 0.02	0.19 ± 0.02	0.34	0.46
τ_{RH}/τ_{RO}	1 ± 0.05	0.79 ± 0.04	1	1
q	2	2	2	1

[a] Italic values were fixed in the fitting procedure. [b] Reference 21. [c] Reference 4.

Morgan theory was used in the data analysis for the calculation of electron spin relaxation rates. Here, $1/T_{1e}$ is given by a transient ZFS, described by the trace of the squared ZFS tensor, Δ^2, and a correlation time, τ_v (with activation energy E_v), and a so-called spin-rotation (SR) relaxation term. This SR is related to the rotational correlation time, τ_{RO}, and characterized by the parameter δg_L^2.[4,33] Physically meaningful parameters have been proposed to describe electron spin relaxation in a recent theory involving both transient and static ZFS.[37−39] However, this model could not be used here due to the lack of crucial EPR data. We have to note that intramolecular dipole−dipole interactions between close Gd^{III} centers have been found for similar dinuclear chelates[4] and for dendrimeric complexes[40] by high-field EPR measurements. Although we have no experimental evidence, the existence of such interactions cannot be excluded in our systems. However, as it was previously shown,[40] they definitely do no influence (limit) the proton relaxivities at imaging fields.

In the fitting procedure, r_{GdO} has been fixed at 2.50 Å based on available crystal structures[41,42] and recent EPR results.[43] The Gd^{III}−H distance, r_{GdH}, has been set to 3.10 Å [4,44] the distance of closest approach of an outer-sphere water proton to the gadolinium(III) center, a_{GdH}, to 3.5 Å,[4] and the quadrupolar coupling constant, $\chi(1 + \eta^2/3)^{1/2}$ to the value for pure water, 7.58 MHz. The diffusion constant, D^{298}_{GdH} and its activation energy, E_{DGdH}, used in the analysis of ^1H NMRD data, were fixed to 23×10^{-10} m^2 s^{-1} and 30 kJ mol^{-1}, respectively. The activation energy for the zero field splitting modulation, E_v, had a value of 1 kJ mol^{-1}. For δg_L^2, characterizing the spin-rotation contribution to electronic relaxation, we obtained 0.08 ± 0.01 for both complexes. All parameters obtained in the fitting procedure are given in Table 3.

The value of the ^{17}O scalar coupling constant, $A/\hbar$, is directly determined by the chemical shifts. It is related to the metal−coordinated oxygen distance and usually falls within a limited range for various gadolinium(III) polyaminocarboxylate complexes. The values obtained here for both $[Gd_2(pX(DTTA)_2)(H_2O)_4]^{2-}$ and $[Gd_2(mX(DTTA)_2)(H_2O)_4]^{2-}$, -3.6×10^6 and -3.4×10^6 rad s^{-1}, respectively, are in the usual range,[4,45] which confirms the assumption of two water molecules per Gd^{III} ion in the inner coordination sphere of each complex ($q = 2$).

The gadolinium(III) complexes of both para and meta ligands exhibit similar water exchange behavior. The water exchange rates are identical within experimental error ($k^{298}_{ex} = (9.0 \pm 0.4) \times 10^6$ s^{-1} for $[Gd_2(pX(DTTA)_2)(H_2O)_4]^{2-}$ and $(8.9 \pm 0.5) \times 10^6$ s^{-1} for $[Gd_2(mX(DTTA)_2)(H_2O)_4]^{2-}$). These values are also very close to $k^{298}_{ex} = (8.6 \pm 0.6) \times 10^6$ s^{-1} found for $[Gd(TTAHA)(H_2O)_2]^{3-}$. It is well-known that substituents that do not directly interfere in the inner coordination sphere hardly affect k_{ex}.[32,33,46−48] The replacement of the third pending arm of the tripod TTAHA by an aromatic linker indeed does not modify the water exchange process. On the other hand, the k^{298}_{ex} obtained for the dinuclear chelates is higher than that for $[Gd(DTPA)(H_2O)]^{2-}$ (Table 3). One possible explanation for this difference is the presence of the two water molecules in the inner sphere of the complex which decreases the stereorigidity of the system.[21] Similar k^{298}_{ex} value has been reported for the macrocyclic $[Gd(DO3A)(H_2O)_q]$, which is present in a hydration equilibrium with an average q of 1.9.[49] To the best of our knowledge, the water exchange rates measured for $[Gd_2(pX(DTTA)_2)(H_2O)_4]^{2-}$ and $[Gd_2(mX(DTTA)_2)(H_2O)_4]^{2-}$ are the highest published for dinuclear compounds (Table 4). For $[Gd_2(pi(DTTA)_2)(H_2O)_2]^{2-}$ (Figure 1), which also has

(34) McLachlan, A. D. *Proc. R. Soc. London* **1964**, *A280*, 271.
(35) Powell, D. H.; Merbach, A. E.; González, G.; Brücher, E.; Micskei, K.; Ottaviani, M. F.; Köhler, K.; von Zelewsky, A.; Grinberg, O. Y.; Lebedev, Y. S. *Helv. Chim. Acta* **1993**, *76*, 1.
(36) Rast, S.; Fries, P. H.; Belorizky, E. *J. Chem. Phys.* **2000**, *113*, 8724.
(37) Rast, S.; Borel, A.; Helm, L.; Belorizky, E.; Fries, P. H.; Merbach, A. E. *J. Am. Chem. Soc.* **2001**, *123*, 2637.
(38) Rast, S.; Fries, P. H.; Belorizky, E.; Borel, A.; Helm, L.; Merbach, A. E. *J. Chem. Phys.* **2001**, *115*, 7554.
(39) Dunand, F. A.; Borel, A.; Helm, L. *Inorg. Chem. Commun.* **2002**, *5*, 811.
(40) Nicolle, G. M.; Tóth, É.; Schmitt-Willich, H.; Radüchel, B.; Merbach, A. E. *Chem. Eur. J.* **2002**, *8*, 1040.
(41) Spirlet, M.-R.; Rebizant, J.; Desreux, J. F.; Loncin, M.-F. *Inorg. Chem.* **1984**, *23*, 359.
(42) Stezowski, J. J.; Hoard, J. L. *Isr. J. Chem.* **1984**, *24*, 323.
(43) Raitsimring, A. M.; Astashkin, A. V.; Baute, D.; Goldfarb, D.; Caravan, P. *J. Phys. Chem. A* **2004**, *108*, 7318.
(44) Astashkin, A. V.; Raitsimring, A. M.; Caravan, P. *J. Phys. Chem. A* **2004**, *108*, 1990.
(45) Micskei, K.; Powell, D. H.; Helm, L.; Brücher, E.; Merbach, A. E. *Magn. Reson. Chem.* **1993**, *31*, 1011.
(46) Tóth, É.; Burai, L.; Brücher, E.; Merbach, A. E. *J. Chem. Soc., Dalton Trans.* **1997**, 1587.
(47) Aime, S.; Geninatti Crich, S.; Gianolio, E.; Terreno, E.; Beltrami, A.; Uggieri, F. *Eur. J. Inorg. Chem.* **1998**, 1283.
(48) Tóth, É.; Connac, F.; Helm, L.; Adzamli, K.; Merbach, A. E. *Eur. J. Inorg. Chem.* **1998**, 2017.
(49) Tóth, É.; Dhubhghaill, O. M. N.; Besson, G.; Helm, L.; Merbach, A. E. *Magn. Reson. Chem.* **1999**, *37*, 701.

Table 4. Hydration Number, q, Rotational Correlation Times of the Gd^{III}−O Vector, τ_{RO}^{298} (ps), Water Exchange Rates, k_{ex}^{298} (10^6 s^{-1}) and Longitudinal Proton Relaxivities, r_1 (mM^{-1} s^{-1}; 20 MHz and 37 °C) for Various Gd^{III} Polyaminocarboxylates (for Ligand Structures See Figure 1)

	q	τ_{RO}^{298}	k_{ex}^{298}	r_1	ref
Monomers					
$[Gd(DOTA)(H_2O)]^-$	1	77	4.1	3.8	4
$[Gd(DTPA)(H_2O)]^{2-}$	1	58	3.3	4.0	4
$[Gd(TTAHA)(H_2O)_2]^{3-}$	2	82	8.6	6.6	21
Dimers					
$[Gd_2(pip(DO3A)_2)(H_2O)_2]$	1	171	1.5	5.8	4
$[Gd_2(pi(DTTA)_2)(H_2O)_2]^{2-}$	1	130	1.1	5.3	6
$[Gd_2(bisoxa(DO3A)_2)(H_2O)_2]$	1	106	1.4	4.9	4
$[BO\{Gd(DO3A)(H_2O)\}_2]$	1	250	1.0	4.6	5
$[Gd_2(en(DO3A)_2)(H_2O)_2]$	1	105	1.3	3.6	6
$[Gd_2(pX(DTTA)_2)(H_2O)_4]^{2-}$	2	278	9.0	12.8	this work
$[Gd_2(mX(DTTA)_2)(H_2O)_4]^{2-}$	2	289	8.9	11.6	this work

a linear DTTA Gd^{III}-coordinating moiety, but only one inner-sphere water molecule, a k^{298}_{ex} of only 1.1×10^6 s^{-1} was reported.[6] The activation entropy $\Delta S^{\ddagger}$ and enthalpy $\Delta H^{\ddagger}$ of both dinuclear Gd^{III} complexes point to a dissociatively activated interchange I_d water exchange mechanism, as it was also observed for the nine-coordinate $[Gd(TTAHA)(H_2O)_2]^{3-}$ and $[Gd(DTPA)(H_2O)]^{2-}$.

In the whole range of proton Larmor frequencies, the values of the longitudinal ^1H relaxivity, r_1, of $[Gd_2(pX(DTTA)_2)(H_2O)_4]^{2-}$ and $[Gd_2(mX(DTTA)_2)(H_2O)_4]^{2-}$ are similar and higher than that of commercial MRI contrast agents. This can be mainly accounted for by the presence of two inner-sphere water molecules. In addition, the higher reorientational correlation time of the dinuclear complexes also contributes to the relaxivity increase. Inner- and outer-sphere relaxivity contributions represent around 50−50% for small molecular weight chelates; consequently, for a $q = 2$ complex the relaxivity can be expected to increase by ~50% as compared to an analogue $q = 1$ system ($[Gd(TTAHA)(H_2O)_2]^{3-}$ vs $[Gd(DTPA)(H_2O)]^{2-}$). The r_1 values measured for $[Gd_2(pX(DTTA)_2)(H_2O)_4]^{2-}$ and $[Gd_2(mX(DTTA)_2)(H_2O)_4]^{2-}$ are more than the double of r_1 for the other dinuclear complexes reported in Table 4. This clearly indicates that the slower rotation of our dinuclear chelates as compared to the previously reported, less rigid analogues also contributes to their higher relaxivity. Analogously, higher relaxivities have been also observed for bishydrated $[Gd(TTAHA)(H_2O)_2]^{3-}$ in comparison to monohydrated $[Gd(DTPA)(H_2O)]^{2-}$).[21] On the other hand, the increased water exchange rate with regard to the commercial agents has only a limited beneficial effect, given the relaxivity is mainly limited by fast rotation.

To attain a substantial relaxivity hump at frequencies of commonly used MRI magnets (20−60 MHz), a high molecular weight and an extensive rigidity of the contrast agent must coexist. Both dinuclear complexes display only a little hump (slightly more important for $[Gd_2(pX(DTTA)_2)(H_2O)_4]^{2-}$). Numerous dinuclear complexes have been previously reported,[4−6] but the relaxivity gain brought by their larger molecular size (compared to monomeric species) was cut back by internal flexibility of the molecule: the flexible linking between the two DO3A or DTTA subunits of most of the previously published dinuclear complexes presented in Table 4 prevents a significant increase in r_1 as compared to the commercial parent $[Gd(DOTA)(H_2O)]^-$ and $[Gd(DTPA)(H_2O)]^{2-}$ monomers. In the case of $[Gd_2(pX(DTTA)_2)(H_2O)_4]^{2-}$ and $[Gd_2(mX(DTTA)_2)(H_2O)_4]^{2-}$, the aromatic linker induces a rigidity. However, the methylene group between the benzene ring and the central aliphatic nitrogen atom, which is necessary to ensure a satisfactory thermodynamic Gd^{III} stability (vide supra), introduces a certain flexibility which then limits relaxivity. In the past, the rotational dynamics of several macromolecular systems has been characterized by using the Lipari−Szabo spectral density functions which provide correlation times for the local and global rotation, as well as a correlation parameter between those two motions.[50] The overall size of the dinuclear complexes is, however, not large enough and does not allow for the use of the Lipari−Szabo approach: the ^{17}O longitudinal relaxation rates and their magnetic field independence in particular could be well described by the usual spectral density functions. In such cases, the internal flexibility of the molecule—though it exists—cannot be quantitatively assessed.

Recent studies on the rotation of Gd^{III} chelates showed that the internal motions of the coordinated water must also be taken into account.[51,52] In the simultaneous analysis of the ^{17}O and ^1H relaxation data, the rotational correlation time of the $Gd-O_{water}$ vector, τ_{RO} (influencing ^{17}O $1/T_1$), and of the $Gd-H_{water}$ vector, τ_{RH} (influencing proton r_1), have been separated. The ratio of the two rotational correlation times for different Gd^{III} complexes has been measured experimentally[51] and simulated by molecular dynamics;[52] both methods gave similar values of $\tau_{RH}/\tau_{RO} = 0.65 \pm 0.2$ for monohydrated chelates. In the present analysis, we obtained higher values for this ratio, especially for $[Gd_2(pX(DTTA)_2)(H_2O)_4]^{2-}$ (Table 3). The restricted internal motion of the $Gd-H_{water}$ vector, implied by a ratio close to 1, may arise from the constraints caused by the presence of two adjacent inner-sphere water molecules. In the meta chelate; however, a somewhat closer vicinity of the two Gd^{III} ions may induce electronic repulsions that counterbalance the restricted $Gd-H_{water}$ vector movements. The larger value of the ratio for the para complex, with respect to the meta analogue could be also indicative of a more rigid system and is reflected by the larger relaxivity hump in the 10−200 MHz region of the ^1H NMRD profiles.

The rotational correlation time τ_{RO}^{298} obtained in the fitting procedure is slightly higher for $[Gd_2(mX(DTTA)_2)(H_2O)_4]^{2-}$ than for $[Gd_2(pX(DTTA)_2)(H_2O)_4]^{2-}$ (289 vs 278 ps); and due to a higher molecular weight, it is more than 3 times larger for the dinuclear complexes than for $[Gd(TTAHA)(H_2O)_2]^{3-}$. Although one can only speculate on the origin of the small difference in the rotation of the two dinuclear

(50) Tóth, É.; Helm, L.; Kellar, K. E.; Merbach, A. E. *Chem. Eur. J.* **1999**, *5*, 1202.
(51) Dunand, F. A.; Borel, A.; Merbach, A. E. *J. Am. Chem. Soc.* **2002**, *124*, 710.
(52) Yerly, F.; Hardcastle, K. I.; Helm, L.; Aime, S.; Botta, M.; Merbach, A. E. *Chem. Eur. J.* **2002**, *8*, 1031.
(53) Ruloff, R. Ph.D. Thesis, Universität Leipzig, Leipzig, Germany, 1997.
(54) Martell, A. E.; Motekaitis, R. J.; Clarke, E. T.; Delgado, R.; Sun, Y.; Ma, R. *Supramol. Chem.* **1996**, *6*, 353.

compounds, it is real, as clearly shown by the experimental ^{17}O $1/T_1$ relaxation rates being somewhat higher for the meta isomer. The simultaneous analysis of the ^{17}O and ^{1}H relaxation rates therefore suggests that the small relaxivity difference at high frequencies between the two dinuclear complexes (in favor of the para isomer, contrary to the ^{17}O relaxation rates) originates from a difference in the internal rotation of the water O−H vector. It has to be noted that one cannot exclude a small difference in the Gd−H distance either, which could also result in different proton relaxivities. Indeed, the experimental proton relaxivity data can be well described for both chelates with identical rotational correlation times and slightly different Gd−H distances (r_{GdH} = 3.10 and 3.14 Å for the para and meta isomers, respectively). On the other hand, differences in the electron spin relaxation cannot be responsible for the differing relaxivities, since, at high frequencies, they have limited influence.

Conclusions

We report the synthesis and physicochemical characterization of two new, potential Gd^{III} MRI contrast agents, $[Gd_2(pX(DTTA)_2)(H_2O)_4]^{2-}$ and $[Gd_2(mX(DTTA)_2)(H_2O)_4]^{2-}$, based on a xylene core substituted in either para or meta position by polyaminocarboxylate groups suitable for Ln^{III} complexation. The structure of both ligands is derived from the parent TTAHA.$^{6-}$ The two chelates exhibit high Gd^{III} complex stability which avoids the release of free toxic Gd^{III} ion in the body, thus representing a prerequisite for medical application.

The water exchange rate, which is identical within experimental error for the two isomers, is the highest reported for dinuclear complexes, thanks to the presence of two water molecules in the inner coordination sphere.

The two inner-sphere water molecules in the Gd^{III} complexes, a relatively long rotational correlation time originating from the increased molecular size, as well as a relatively rigid linker between the two polyaminocarboxylate subunits, all contribute to a remarkably high longitudinal proton relaxivity at all ^{1}H NMRD frequencies for both para and meta isomers, when compared to MRI contrast agents and previously published dinuclear compounds.

Acknowledgment. We thank Dr. Robert Ruloff for helpful discussions and advice. We are grateful to Prof. Manfred Mutter, Dr. Alain Razaname, and Anne-Lise Carrupt for their help with the ESI-MS. The Swiss National Science Foundation is acknowledged for financial support. This research was carried out in the frame of the European-funded EMIL program (Grant LSHC-2004-503569) and the EU COST Action D18.

Supporting Information Available: ^{1}H NMR spectra of $[pX(DTTA)_2]^{8-}$ and $[mX(DTTA)_2]^{8-}$ titration curves of the $[mX(DTTA)_2]^{8-}$ ligand and its Gd^{III}, Zn^{II}, and Ca^{II} complexes, variable-temperature UV−vis absorbance spectra of $[Eu_2(pX(DTTA)_2)(H_2O)_4]^{2-}$ and $[Eu_2(mX(DTTA)_2)(H_2O)_4]^{2-}$, proton relaxivities, transverse and longitudinal ^{17}O relaxation rates, and chemical shifts of $[Gd_2(pX(DTTA)_2)(H_2O)_4]^{2-}$ and $[Gd_2(mX(DTTA)_2)(H_2O)_4]^{2-}$ as a function of magnetic field and temperature, equations used in the data treatment (PDF). This material is available free of charge via the Internet at http://pubs.acs.org.

IC0500309